

1 Evolution of host resistance towards pathogen exclusion: the role of predators.

2
3 Andy Hoyle¹, Alex Best^{2,3}, Roger G. Bowers⁴

4
5 ¹ School of Natural Sciences, University of Stirling, Stirling, FK9 4LA, UK.

6
7 ² School of Mathematics and Statistics, University of Sheffield, Sheffield, S3 7RH, UK.

8
9 ³ Biosciences, College of Life and Environmental Sciences, University of Exeter, Cornwall Campus, Penryn,
10 TR10 9EZ, UK.

11
12 ⁴ Department of Mathematical Sciences, The University of Liverpool, Liverpool, L69 3BX, UK.

13
14 Corresponding Author: A. Best. Tel: +44 1142223704, Email: a.best@shef.ac.uk

15
16
17 Abstract

18 Question: Can increased host resistance drive a pathogen to extinction? Do more complex ecosystems
19 lead to significantly different evolutionary behaviour and new potential extinctions?

20 Mathematical Method: Merging host parasite models with predator prey models. Analytically studying
21 evolution using adaptive dynamics and trade-off and invasion plots, and carrying out numerical
22 simulations.

23 Key Assumptions: Mass action (general mixing). All individuals of a given phenotype are identical. Only
24 prey vulnerable to infection. Mutations are small and rare (however the assumption on the size of
25 mutation is relaxed later). In simulations, very small (negligible) populations are at risk of extinction.

26 Conclusions: The presence of the predator can significantly change evolutionary outcomes for host
27 resistance to a pathogen and can create branching points where none occurred previously. The
28 pathogen (and sometimes the predator) is protected from exclusion if we take mutations to be
29 arbitrarily small; however relaxing the assumption on mutation size can lead to its exclusion. Increased
30 resistance can drive the predator and/or pathogen to extinction depending on inter-species dynamics,
31 such as predator's preference for infected prey. Predator co-evolution can move exclusion boundaries
32 and prevent the predator's own extinction if its rate of mutation is high enough (in respect to the
33 prey's).

34
35 Keywords: adaptive dynamics, co-evolution, extinction, eco-epidemiology, parasite, singular strategy.

36 1) Introduction

37
38 Understanding the evolutionary dynamics of infectious diseases remains a key topic in evolutionary
39 ecology and is central to our management of natural systems. Our theoretical understanding of the
40 evolution of hosts and their parasites continues to grow (e.g. Levin and Pimental, 1981; Boots and
41 Haraguchi, 1999; Best et al., 2010), yet studies tend to assume that hosts and parasites interact in
42 isolation. In reality, ecosystems consist of a complex mix of species, including hosts, parasites, predators,
43 prey, competitors and mutualists. Understanding how infectious disease dynamics are affected by the
44 interference of this range of interacting species is clearly crucial for any predictions to be made in real
45 systems.

46
47 Much of the theory on infectious disease systems has focussed on the evolution of the parasite,
48 investigating, for example, when disease may become endemic and when highly virulent parasites may
49 be selected for (e.g. Levin and Pimental, 1981; Anderson and May, 1981; Pugliese, 2002; Svernungsen
50 and Kisdi, 2009). In response to parasitism, hosts are clearly likely to experience strong selection to
51 develop defence mechanisms, and there is a growing body of theory focussing on the evolution of the
52 host (e.g. Frank, 1993; Boots and Bowers, 1999, 2004). Broadly, host defence may be divided into two
53 sub-classes: resistance and tolerance. Resistance mechanisms, which act to directly harm the parasite,
54 include avoidance of infection (Boots and Haraguchi, 1999; Boots and Bowers, 1999), clearance of
55 disease (Boots and Bowers, 1999; van Baalen, 1998) and acquired immunity (Boots and Bowers, 2004),
56 whilst tolerance mechanisms do not affect the parasite, but rather ameliorate parasite-induced damage
57 (Boots and Bowers, 1999, 2004; Roy and Kirchner, 2000; Miller et al., 2005). The differing feedbacks
58 produced by these alternate defence mechanisms can result in very different behaviours (Boots, 2008;
59 Boots et al., 2009), for example allowing branching to coexistence of host strains when defence is
60 through resistance but not when it is through tolerance (Roy and Kirchner, 2000; Miller et al., 2005; but
61 see Best et al., 2009).

62
63 Whilst the evolution of both parasites and hosts (and, increasingly, their co-evolution (van Baalen, 1998;
64 Dieckmann et al., 2002; Restif and Koella, 2003; Best et al., 2010) is now well studied in relatively simple
65 one host – one parasite systems, there has been little consideration of how interactions with other
66 species may impact disease dynamics. Conversely, a number of predator-prey and competition models
67 have shown that interacting species play an important role in their evolutionary dynamics (e.g. Bowers
68 et al., 2003; Kisdi, 1999; Hoyle et al., 2008), however these do not include pathogens. In two recent
69 exceptions, Morozov and Adamson (2011) and Morozov and Best (In Press) studied an SI model where
70 predators fed on infected prey and found that the evolution of pathogen virulence changes due to the
71 presence of a predator. In population studies, extensive studies have shown that these interactions,
72 particularly predate-prey-infection (or eco-epidemiological) models, can have significant effects on the
73 dynamics of species and on disease control strategies (e.g. Venturino, 2001, 2002; Haque et al., 2009;
74 Greenman and Hoyle, 2010; Haque and Greenhalgh, 2010; Hudson and Greenman, 1998). These include
75 unbalancing competitive effects and driving one species to extinction, or in some cases allowing two
76 species to co-exist where they would usually not be able to (Hudson and Greenman, 1998).

77

78 Much of the modern literature on the evolutionary ecology of hosts and parasites has been conducted
79 within the framework of adaptive dynamics (Metz et al., 1996a; Geritz et al., 1998), which allows the
80 study of trait substitution sequences resulting from the challenge of a resident strain by a closely similar
81 mutant. One key feature of most of these studies is the evolutionary trade-off between beneficial
82 mutations (for example, increased defence in the host) and fitness costs incurred elsewhere (for
83 example, reduced reproductive ability). The shape of these evolutionary trade-offs has been found to be
84 crucial to the outcomes of a range of ecological systems, and is now central to much of adaptive
85 dynamics theory (de Mazancourt and Dieckmann, 2004; Rueffler et al., 2004; Bowers et al., 2005).
86 Focussing on host evolution, where defence comes at accelerating costs – i.e. each additional unit of
87 benefit is met by an increased cost – the system generally tends to an intermediate strategy which is a
88 long-term attractor of evolution (or a Continuously Stable Strategy), whereas where defence incurs
89 decelerating costs hosts may be driven to maximise or minimise defence due to an evolutionary
90 repeller. Trade-offs that are weakly accelerating or decelerating (or even linear) may display either
91 behaviour, or may exhibit evolutionary branching, where the initial monomorphic population splits in to
92 two (or more) coexisting strains.

93
94 The major aim of this paper is to investigate the relevance of the relationship between trade-offs and
95 evolutionary outcomes in the context of the evolution of host resistance to parasitism in the presence of
96 an immune predator. In particular we look into what trade-off shapes enhance the possibility of co-
97 existence between species, potentially leading to branching and speciation, and what shapes lead to
98 significant changes in the ecosystem with the eradication of pathogens and/or predators. We use the
99 method of Trade-off and Invasion Plots (TIPs) (Bowers et al., 2005), which highlights the role of the
100 trade-off in determining the evolutionary outcome, and thus intend to show the efficacy of this
101 approach in such investigations. We also carry numerical simulations which allow the inclusion of some
102 stochastic behaviour. We initially take a prey only system, modelled by a standard SIS (susceptible-
103 infected-susceptible) model and investigate the evolutionary behaviour of the system when host
104 resistance (through decreased transmission) is costly to an aspect of the disease free demography
105 (decreased birth rate). In particular we look at whether evolution of the host can exclude the pathogen.
106 We then move on to include the immune predator in the system and look at how the evolutionary
107 behaviour changes and if the predator can be excluded from the system. We initially do this by looking
108 at evolution of the prey alone, before moving onto a co-evolutionary set-up where the prey and
109 predator co-evolve.

110

111 2) The Model

112

113 Our analysis is based on a predator-prey system where the prey is subject to a pathogen, modelled by
 114 an SIS set-up, but the predator is immune. We use the equations

115

$$\frac{dS}{dt} = aH - qH^2 - bS - \beta SI + \gamma I - cSP$$

$$116 \quad \frac{dI}{dt} = \beta SI - (\alpha + b + \gamma)I - c\phi IP \quad (1)$$

$$\frac{dP}{dt} = \theta cP(S + \phi I) - dP$$

117

118 where S and I are the densities of susceptible and infected prey, with $H = S + I$, and P is the
 119 density of predators. In addition, a is the prey birth rate, q is the rate of density dependence
 120 competition (acting on births), b is the natural prey death rate, β is the transmission rate, α is the
 121 parasite induced death rate or pathogenicity, γ is the recovery rate, c is the predation rate, ϕ
 122 represents the increase/decrease in predation rate suffered by infected individuals, θ relates to the
 123 conversion of predation into the births of new predators and d is the predator death rate.

124

125 3) Pathogen Exclusion - Evolution of resistance in a prey-only environment

126

127 We stress here that although we are taking $c = 0$ throughout this section, we leave it in the respective
 128 equations as we will later take $c > 0$ and refer back.

129

130 With respect to prey evolution and the algebraic analysis throughout this study, we assume that the
 131 host can evolve resistance to parasitism through reducing the transmission rate, β . Due to constraints,
 132 such as energetic ones (resource allocation), any benefit gained in one life-history trait must come at the
 133 cost of another and hence we assume a cost to resistance through reduced birth rate, with a trade-off
 134 $a = f(\beta)$ with $f' > 0$. We take the trade-off to be of the form:

135

$$136 \quad a = f(\beta) = f(1) - \frac{f'(1)^2}{f''(1)} \left(1 - e^{\frac{f''(1)}{f'(1)}(\beta-1)} \right) \quad (2)$$

137

138 In each example, the value of $f'(1)$ is chosen to ensure there is always a singular strategy at $\beta^* = 1$,
 139 with $a^* = 2$. (We see similar results for other choices.) All other parameters are taken to be constant.
 140 We take a and β to represent the traits of the resident strain, existing at a stable equilibrium with
 141 densities $S = S(a, \beta)$ and $I = I(a, \beta)$, (later coexisting with a predator at density $P = P(a, \beta)$), and
 142 \hat{a} and $\hat{\beta}$ to represent the traits of the mutant strain. If we were to draw up the dynamics for $d\hat{S}/dt$

143 and $d\hat{I}/dt$ of the mutant population, the invasion part of the Jacobian matrix, evaluated at the resident
 144 only equilibrium, would be

$$145 \quad \begin{pmatrix} \hat{a} - qH - b - \hat{\beta}I - cP & \hat{a} - qH + \gamma \\ \hat{\beta}I & -\Gamma - c\phi P \end{pmatrix} \quad (3)$$

147 where $\Gamma = \alpha + b + \gamma$. The fitness is given by the maximum eigenvalue of this matrix (Metz et al., 1996a;
 148 Geritz et al., 1998), however we can derive a sign equivalent form of the fitness, which we hereafter call
 149 the fitness for convenience, as the negative of the determinant of this matrix (see Appendix A for proof),
 150 i.e.

$$151 \quad s(\hat{a}, \hat{\beta}; a, \beta) = (\hat{a} - qH - b - \hat{\beta}I - cP)(\Gamma + c\phi P) + \hat{\beta}I(\hat{a} - qH + \gamma) \quad (4)$$

152 (We have not yet included the trade-off.) We use the method of trade-off and invasion plots to analyse
 153 the evolutionary behaviour. Here we calculate two invasion boundaries: the f_1 invasion boundary, of
 154 the form $\hat{a} = f_1(\hat{\beta}, \beta)$ derived from $s(\hat{a}, \hat{\beta}; a, \beta) = 0$ (taking $a = f(\beta)$), which separates the $(\hat{a}, \hat{\beta})$ -
 155 space into regions where a mutant with traits $(\hat{a}, \hat{\beta})$ can and cannot invade a resident with traits
 156 (a, β) , and the f_2 invasion boundary, of the form $\hat{a} = f_2(\hat{\beta}, \beta)$, derived from $s(a, \beta; \hat{a}, \hat{\beta}) = 0$
 157 (again taking $a = f(\beta)$), which separates the $(\hat{a}, \hat{\beta})$ -space into regions where a mutant with traits
 158 (a, β) can and cannot invade a resident with traits $(\hat{a}, \hat{\beta})$.

159 An evolutionary singularity occurs when the trade-off $\hat{a} = f(\hat{\beta})$ is tangential to the invasion boundaries
 160 at the point $(\hat{a}, \hat{\beta}) = (a, \beta)$ (the two invasion boundaries are always tangential at that point). The
 161 relative curvatures of the trade-off and the two invasion boundaries, evaluated at an evolutionary
 162 singularity, determine the evolutionary properties of that singularity, in particular evolutionary stability
 163 (ES) – whether a singularity can be invaded – and convergence stability (CS) – whether species will
 164 evolve towards or away from a singularity. (See Appendix B for full details and workings.) Combinations
 165 of these determine the nature of the evolutionary singularity. It can be: an evolutionary attractor (CSS) if
 166 it is ES and CS, an evolutionary branching point if it is CS but not ES, or an evolutionary repellor (in which
 167 we also include a ‘Garden of Eden’ point or ES-repellor) if it is not CS (the ES status is then mostly
 168 irrelevant).

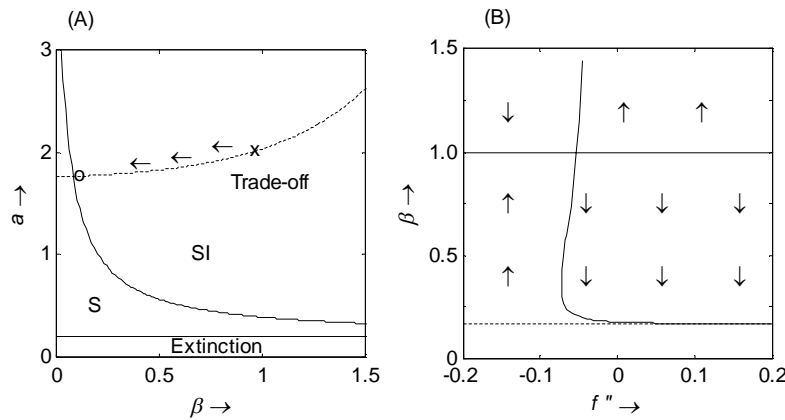
169 In our model, it is possible for the evolutionary singularity to exhibit any of the long-term behaviour
 170 mentioned above, depending on the choice of parameter values and trade-off shape.

171 We find that especially interesting behaviour occurs in the model if the singularity (specifically the
 172 singularity at $\beta^* = 1$) is an evolutionary repellor, and the prey is initially below (lower β) the singular

179 point. Here the prey evolves away from the singularity towards an extreme state of high resistance (i.e.
 180 low transmission), which will move the system towards a point where the pathogen is excluded. This
 181 exclusion (or invasion) threshold for infection (although we are assuming a predator-free environment
 182 we have left c in for results later), is given by

$$184 \quad R_{0I} = \frac{\beta S_{XI}}{\alpha + b + \gamma + c\phi P_{XI}} = 1 \quad (5)$$

185
 186 where S_{XI} (and P_{XI}) represent the equilibrium density of the prey (and predator) in the absence of the
 187 pathogen. This threshold (along with the host extinction threshold given by $a = b$) is plotted in trade-off
 188 space in Figure 1A. If the prey evolves to a point where the reproduction ratio R_{0I} in (5) is less than 1,
 189 then the pathogen can be excluded from the environment. (This may not be the case in more complex
 190 model set-ups where backwards bifurcations can occur – in that case invasion and exclusion boundaries
 191 can be different. However here, and in all simulations throughout our study, backwards bifurcations do
 192 not occur.) However analysis about this point of exclusion reveals some interesting conclusions.
 193



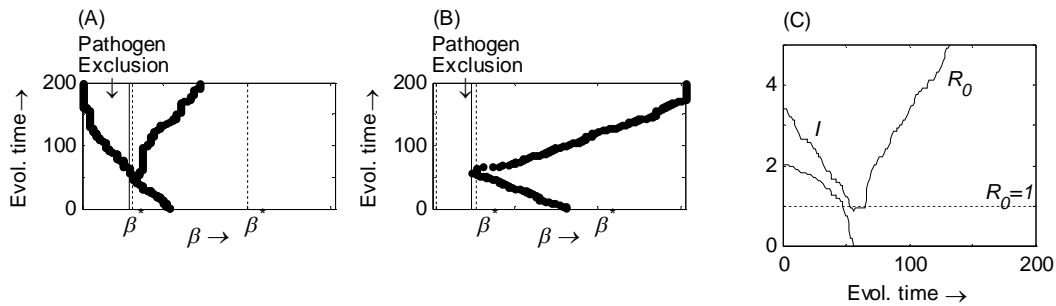
194
 195
 196 Fig. 1: In (A) we plot the exclusion threshold $R_{0I} = R_0 = 1$ in trade-off space. The letters in each region
 197 denote the species that would be present (have positive density): S=uninfected prey only, SI=infected
 198 co-existence. The lower extinction threshold is when the prey birth rate falls below the natural death
 199 rate. The trade-off (dashed line) corresponds to that in Fig, 2B, where "o" denotes the CS singularity, "x"
 200 represents repellor singularity and the arrows the direction of evolution before pathogen exclusion. In
 201 (B) we plot the singularities β^* for different trade-off curvatures. The dashed curve represents the
 202 exclusion threshold, and the arrows represent the direction of evolution with respect to β . The
 203 parameter values are $q = 0.5$, $b = 0.2$, $\alpha = 0.2$, $\gamma = 0.2$, $c = 0$, $\theta = 1$, $d = 0.3$, $\phi = 3$.

204
 205
 206 It is clear that in the absence of infection the prey will evolve to maximise the birth rate a , since the cost
 207 of a higher infection rate, β , is irrelevant. We therefore have a positive fitness gradient when $l=0$. In

208 contrast if, with infection present, the prey evolves higher resistance (lower β) and correspondingly a
209 lower birth rate, then the fitness gradient is negative. Hence there must be a change of sign in this
210 fitness gradient near (just above) the exclusion boundary. Consequently, this change in sign means a
211 singularity must be present before the exclusion boundary is reached – furthermore, given the sign of
212 the fitness gradient either side, we conclude this singularity must be convergent stable (CS) (i.e. an
213 evolutionary attractor or branching point.) We can confirm this by plotting the location of the
214 singularities as we vary the trade-off curvature via $f''(1)$ (Figure 1B). Given a trade-off with an
215 appropriate curvature, the singularity near the exclusion boundary can be a branching point. A
216 numerical simulation for this is shown in Figures 2A (see Appendix C for details of how these simulations
217 were carried out). Here the prey evolves higher resistance, to a point where β is close to the exclusion
218 boundary. The singularity, which is CS but not ES, then causes the population to branch and the two
219 branches to evolve away from each other. Although one branch has passed beyond the exclusion
220 boundary, the presence of the other strain (with increasing β) maintains the infection.

221
222 It is interesting to note that the lower singularity asymptotes towards the exclusion boundary, getting
223 closer as the trade-off curvature gets larger (Figure 1B). Theoretically, according to adaptive dynamics,
224 this protects the pathogen from ever being excluded from the system as, assuming small, rare mutations
225 selection cannot drive the population across the exclusion boundary and the infected population to zero
226 (although, when the singularity is near the boundary, the pathogen will exist only at very low levels).
227 This initially occurs in our numerical simulations in Figure 2B (and subsequent figures later in the paper).
228 Here we plot the evolution of β given that the evolutionary singularity at $\beta^* = 1$ is a repeller. Initially
229 β evolves away from the singularity and towards the lower singularity just above the exclusion
230 threshold (Figure 2B). As this is an attractor, it ‘stops’ here, near this singularity. However, this is
231 temporary, the simulations then go on to exhibit further evolutionary behaviour. In the more realistic
232 case where mutations are not arbitrarily small, when the singular point is sufficiently near the threshold,
233 a mutant which does not itself support the pathogen can arise. This resistant strain cannot remove the
234 pathogen from the system deterministically (it cannot truly invade in the sense of adaptive dynamics).
235 However, its presence suppresses the infection further, essentially to negligible levels, and we find it can
236 take the resident a very long time to out-compete this mutant strain; hence a strain below the threshold
237 is temporarily present in our simulations in Figure 2B. During this time the infection levels continue to
238 fall due to the presence of these resistant mutants below the threshold. We recognize that stochastic
239 effects occur in nature and correspondingly employ them in our simulations. Thus as the infection falls,
240 it becomes prone to stochastic extinction. The simulations therefore deviate from adaptive dynamics
241 theory; they incorporate the fact that at low levels the infection (and in fact any population component
242 with low enough density) has a high probability of extinction. Here we indeed find that infection levels
243 reach such negligible levels for a sustained period of time and may easily be driven to extinction by
244 stochastic effects, and as such it is removed from the simulations (Figure 2C). Of course the probability
245 of this extinction is much enhanced by the fact that the lower singularity is near the exclusion threshold
246 and supports only a very low level of infection. After extinction of the pathogen, any benefit, through
247 higher resistance, the mutant has will be lost and subsequent mutants that arise will be uninfected and

248 a new evolutionary path will be followed, with $S = S_{X_I}$ and $I = 0$. The prey evolves to maximise the
 249 birth rate a without encountering any further singularities (β which is also maximised only affects the
 250 fitness via the trade-off and is not selected upon). However, since at these higher transmission rates,
 251 the population dynamic equilibria are such that $R_0 > 1$, the prey will be vulnerable to future outbreaks by
 252 the pathogen and to returning to the endemic state.
 253



254
 255 Fig. 2: (A+B) Numerical simulations of the evolution of β with a trade-off of the form $a = f(\beta)$, from
 256 (2), where $f''(1) = -0.05$ in (A), and $f''(1) = 1.25$ in (B), both giving rise to an evolutionary repeller at
 257 $\beta^* = 1$. Here β evolves away from this singularity and towards the singularity just above the exclusion
 258 threshold. In (A) this singularity is a branching point and in (B) it is an attractor. In (B) it temporarily
 259 settles at the lower singularity, however random (non-negligible) mutations take β across the
 260 threshold. When it crosses the pathogen exclusion threshold the infected prey density drops to zero.
 261 (See end of section 3 for full details.) (C) Plot of the infected equilibrium density I and the reproduction
 262 ratio R_0 (R_{0_I} with $c = 0$), as given in (5), at each evolutionary step are for the simulation shown in (B).
 263 The infected density, I , reaches negligible levels when the reproduction ratio falls below 1, and is
 264 subsequently in danger of extinction. Due to the exclusion of the pathogen, and hence the change in
 265 selection pressure, β now increases to the upper limit in order to maximise reproduction a . The
 266 parameter values are $q = 0.5$, $b = 0.2$, $\alpha = 0.4$, $\gamma = 0.2$, $c = 0$, $f'(1) = 0.078$.

267
 268

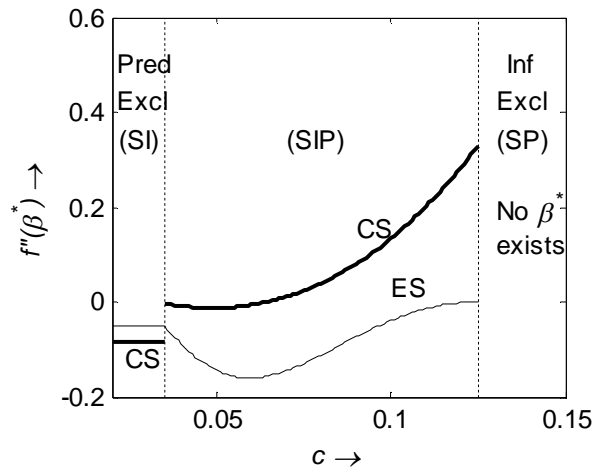
269 4) Evolution of resistance in the presence of a (non-evolving) predator

270

271 Evolutionary effects of the predator

272

273 We again consider a trade-off between the transmission rate, β , and the birth rate, a , however we
 274 now assume a predator is present and take $c > 0$ in (1). The fitness is that in (4). The introduction of the
 275 predator immediately increases the dimension of the feedback environment. Consequently this can
 276 produce significant shifts in evolutionary behaviour such that a singularity that was a repellor (non-CS)
 277 can become convergent stable (an attractor or branching point) without the need to change any other
 278 parameter values or trade-off. In Figure 3 we plot the boundaries for the ES and CS properties, in terms
 279 of the trade-off curvature at the singularity at $\beta^* = 1$, as we vary the rate of predation. If c is too low
 280 the predator is excluded from the environment, and the system returns to that in the previous section,
 281 and if c is too high the pathogen is excluded in which case the prey maximise their birth rate as there is
 282 no cost in terms of a lower resistance. However for intermediate values of c , where the prey, pathogen
 283 and predator co-exist, the general trend is that the size of the branching region between the two
 284 boundaries (by size we mean range of values of the trade-off curvature which produce a branching
 285 point) increases as c increases.
 286



287

288 Fig. 3: The trade-off curvature $f''(1)$ needed to satisfy ES (thin line) and CS (thick line) conditions, for
 289 the singularity at $\beta^* = 1$, (where below each boundary corresponds to satisfying the relevant property)
 290 for a range of values of c . Below both lines denotes an attractor, above the CS line a repellor and
 291 between the two (when the CS line is above the ES line) a branching point. The letters in brackets
 292 denote the species which is present: S=susceptible prey, I=infected prey and P=predator. The parameter
 293 values are $q=0.5$, $b=0.2$, $\alpha=0.2$, $\gamma=0.2$, $a^*=2$, $\beta^*=1$, $\theta=1$, $d=0.3$, $\phi=3$.

294

295

296 We briefly draw attention to the discontinuity in the CS boundary during the transition from a predator-
 297 free environment to a predator-prey-infection environment in Figure 3. This discontinuity is caused by
 298 the way the population densities at the demographic attractor (equilibrium) change through the

299 transition. Although this is continuous (e.g. P goes towards zero as c passes (decreases) through the
 300 transition), it is not smooth. This results in a discontinuity in the gradient of the densities at the
 301 attractor, i.e. in $\partial S / \partial \beta$, $\partial I / \partial \beta$ and $\partial P / \partial \beta$ - this can be seen by the difference in $\partial S / \partial \beta$ through
 302 this point as shown in (D.1); similar differences are present in the I and P derivatives. This in turn
 303 causes a discontinuity in the CS boundary as this depends on the mixed derivative $\partial^2 s / \partial \beta \partial \hat{\beta}$, which in
 304 turn depends on the above gradients. Conversely the ES boundary is continuous but not smooth, as this
 305 depends only on the densities (which are continuous but not smooth) and not on their gradients. (See
 306 Hoyle et al (2011), which explains this behaviour for a discrete time system in more detail.)

307

308

309 Predator and Pathogen Exclusion Thresholds

310

311 Critically in this system there exists not only a pathogen exclusion threshold, as given by equation (5)
 312 (where c is non-zero now), but also a predator exclusion threshold. This bounds a parameter region
 313 where the predator cannot survive. For our model (1) this is given by

314

$$315 \quad R_{0P} = \frac{\theta c}{d} (S_{XP} + \phi I_{XP}) = 1 \quad (6)$$

316

317 where S_{XP} and I_{XP} represent the equilibrium densities of the prey in the absence of the predator. This
 318 is equivalent to the requirement that the number of offspring a single predator would produce over its
 319 lifetime in an entirely prey environment – equivalent to the reproduction number – needs to be greater
 320 than one for the predator to establish. If evolution were to drive this predator ratio below 1 then the
 321 predator could not survive and would be driven extinct. (Again backwards bifurcations do not occur here
 322 and so invasion and exclusion boundaries are equivalent.) Subsequent evolution of resistance by the
 323 prey would be determined in the predator-free environment (as P would remain zero), and hence as
 324 discussed in section 3.

325

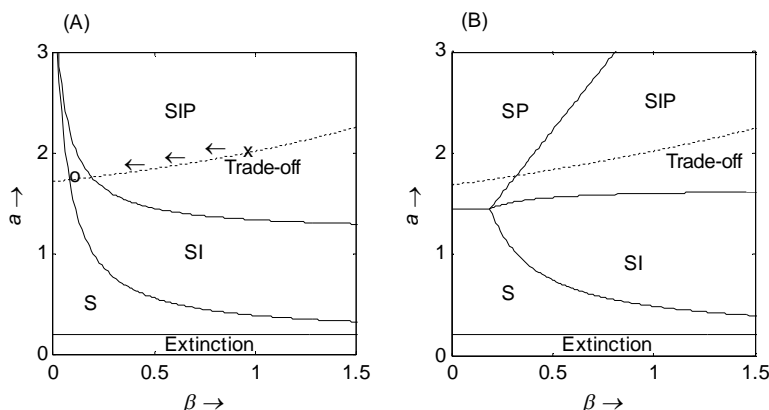
326 Thresholds for when the predator and pathogen will be excluded under different scenarios can be
 327 derived. Combining these we can plot these thresholds in trade-off space. (We note that these
 328 boundaries are independent of the explicit functional form of the trade-off.) Figure 4 shows two
 329 examples, for primarily different values of ϕ (the change in the predation due to prey being infected).

330 In Figure 4A, with $\phi = 3$ i.e. infectious prey are more vulnerable to predation, the trade-off intersects
 331 three separate regions; starting in a predator-prey-infection environment, moving down the trade-off, in
 332 the direction of higher resistance (lower β), first leads to the exclusion of the predator and later the
 333 exclusion of the pathogen. In Figure 4B, with $\phi = 0.8$ i.e. infectious prey are less vulnerable to
 334 predation, gaining higher resistance (moving down the trade-off) will lead to the exclusion of the
 335 pathogen but not the predator. In general, whether the pathogen or predator is excluded first (or at all)

336 depends on which ratio, R_{0p} or R_{0l} , falls below 1 first, with each of them depending on a range of
 337 parameters.

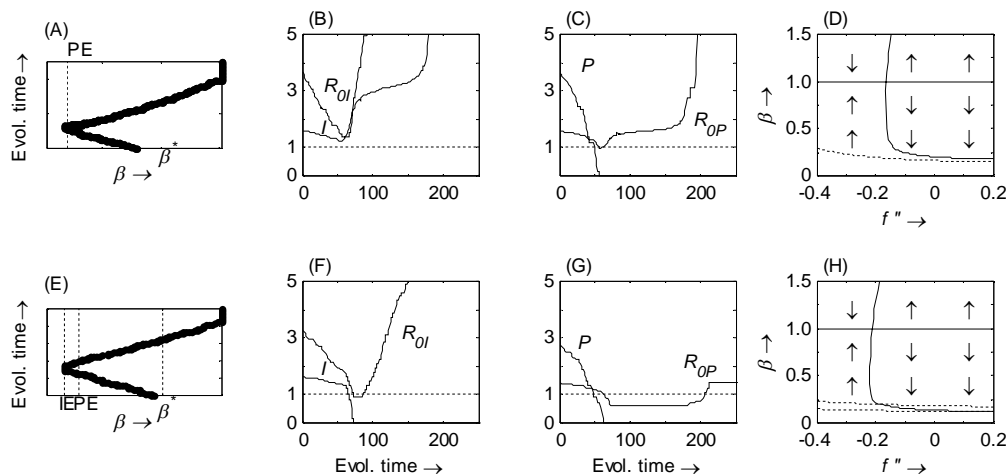
338
 339 Numerical simulations of the evolution of resistance for the case where the singularity at $\beta^* = 1$ is an
 340 evolutionary repeller are shown in Figure 5, where we focus on the situation described in Figure 4A.

341
 342 First we focus on Figures 5A-5D. Here the singularity leads β to evolve to the lower extreme value.
 343 However there is a CS singularity at the threshold, now protecting the predator from exclusion (Figure
 344 5D). This singularity in fact asymptotes towards the predator exclusion boundary but will never cross it.
 345 The reason for this lies in the fact that here $\alpha = 0.0$. Hence, when the predator is excluded, there is no
 346 cost in the prey being infected (as there is no castration, no increased death rate and, with the predator
 347 excluded, no change in predation). Therefore the prey will evolve to maximise its birth rate, with a
 348 higher β giving no cost – i.e. it will have a positive fitness gradient. This positive fitness gradient below
 349 the threshold prevents the singularity from ever passing the threshold (similarly to the pathogen
 350 exclusion case). However once the prey reaches the singularity at the threshold, the predator will only
 351 exist at very low numbers at this singularity, with the predator ratio, R_{0p} in (6), lying just above 1. Here
 352 a combination of non-arbitrarily small mutations and the exclusion of strains at very low density will
 353 again lead to the extinction of the predator (as in the case of the pathogen at the end of section 3)
 354 (Figure 5C). After this point the change in selection pressure mentioned above causes β to increase and
 355 the infection is maintained in the environment. Again it should be noted that this will leave the prey
 356 vulnerable to future predator invasions.



357
 358 Fig. 4: Two plots of the exclusion boundaries given in (5) and (6) in trade-off space, with a trade-off
 359 between the prey reproduction rate and infection rate, $a = f(\beta)$ (with $f''(1) = 1.25$). The dashed line
 360 in (A) represents a given trade-off used in Figures 5E-H. We plot an equivalent trade-off in (B) just for
 361 comparison. The letters in each region denote the species that would be present (have positive density).
 362 S=uninfected prey only, SI=infected prey, SIP=infected prey and predator, SP=uninfected prey and
 363 predator. (Assumes we start from an SIP ($S>0, I>0, P>0$) environment.) The parameter values are
 364 $q = 0.5, b = 0.2, \alpha = 0.2, \gamma = 0.2, c = 0.05$ in (A), $c = 0.12$ in (B) $\theta = 1, d = 0.3, \phi = 3$ in (A),
 365 $\phi = 0.8$ in (B), $f'(1) = 0.0935$ in (A) and $f'(1) = 0.0345$ in (B).

366



367
 368 Fig. 5: Numerical simulations of the evolution of β with a trade-off of the form $a = f(\beta)$ (from (2))
 369 with $f''(1) = 1.25$. Here the singularity at $\beta^* = 1$ is an evolutionary repeller. These simulations are run
 370 for two values of the pathogen induced death rate α , 0 in (A-D) and 0.2 in (E-H). In (A) and (E) we show
 371 the evolution of β , where IE=infection exclusion threshold and PE=predator exclusion threshold. In (B)
 372 and (F) we plot the infection density I at each evolutionary time step along with the ratio R_{OI} , as given
 373 in equation (4). In (C) and (G) we plot the predator density P at each evolutionary time step along with
 374 the ratio R_{OP} , as given in equation (6). In each case, a ratio of below 1 leads to the extinction of the
 375 infection or predator. In (D) and (H) we plot of the location of the evolutionary singularities for various
 376 shapes of trade-off. The dashed line represents the predator exclusion boundary $R_{OP} = 1$, as given in
 377 equation (6), and the lower dashed line in (H) represents the infection threshold $R_{OI} = 1$. The
 378 parameter values are $q = 0.5$, $b = 0.2$, $\gamma = 0.2$, $c = 0.05$, $\theta = 1$, $d = 0.3$, $\phi = 3$, $f'(1) = 0.0935$
 379 in (A-D) and $f'(1) = 0.114$ in (E-H).

380
 381
 382 In contrast, in Figures 5E-5H, with a small change in α from 0 to 0.2 (i.e. an increase in the pathogen
 383 induced death rate), the lower singularity can now, and does, pass below the predator exclusion
 384 threshold (Figure 5H) and in this case asymptotes towards the pathogen exclusion threshold. Here the
 385 predator will inevitably be excluded deterministically (this can occur with the standard small, rare
 386 mutations of adaptive dynamics). The situation changes such that once the prey has crossed the
 387 predator exclusion boundary, and the predator is excluded, the prey continues to evolve in a way that
 388 leads β to decrease and the infection is subsequently excluded as the prey crosses the infection
 389 exclusion threshold in the manner described previously, Figures 5E-5H. After this point, the infection-
 390 free environment changes the selection pressure such that higher β comes at no cost and the prey
 391 subsequently evolves to maximise the birth rate a . Again this leaves the prey vulnerable to future
 392 invasion from both the predator and the pathogen.

393
394395 5) Co-evolution of prey and predator

396

397 We now expand on the situation above, where the prey evolves in such a way to drive the predator to
 398 extinction (Figure 5); we now let the predator evolve too and investigate whether this co-evolutionary
 399 set-up allows the predator to survive. We focus on the situation (Figure 5A-D) where the prey evolved to
 400 decrease β which eventually excluded the predator and an infected prey-only system remained; this is
 401 the only case we consider here.

402

403 We take the predation rate, c , and predator death rate, d , to evolve and suppose that they are linked
 404 by a trade-off of the form $d = g(c)$. The fitness of a rare mutant predator, with traits (\hat{c}, \hat{d}) , attempting
 405 to invade an established resident, with traits (c, d) , in a stable equilibrium with densities S, I, P ,
 406 where the prey has traits (a, β) , is given by

407

$$408 \quad r(\hat{c}, \hat{d}; c, d, a, \beta) = \theta \hat{c}(S + \phi I) - \hat{d} \quad (7)$$

409

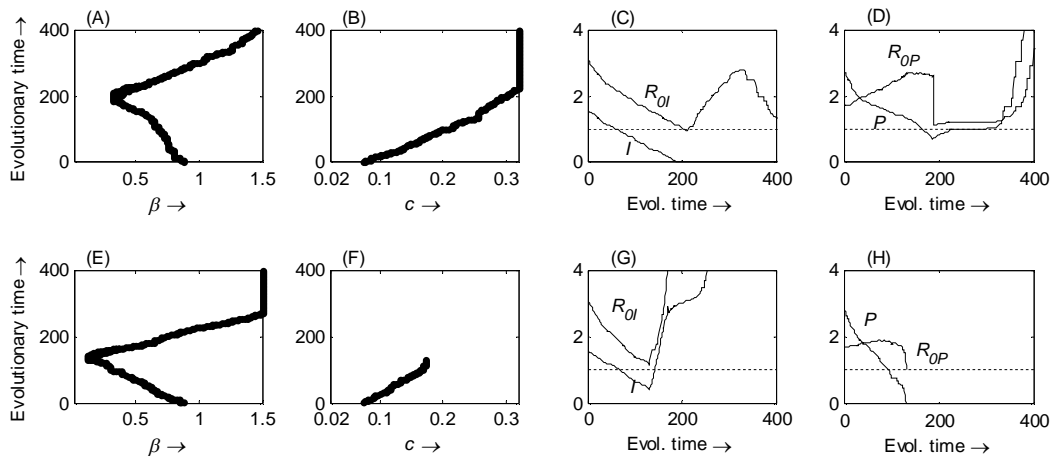
410 (Correspondingly, the fitness of (4) is now best denoted $s(\hat{a}, \hat{\beta}; a, \beta, c, d)$.) Under this model and
 411 trade-off, the predator's evolutionary behaviour follows that of an optimisation set-up, whereby
 412 $(S + \phi I)$ is minimised, and subsequently any singularity is an evolutionary attractor for acceleratingly
 413 costly trade-offs, or an evolutionary repeller for deceleratingly costly trade-offs – branching points are
 414 not possible. (For full details on this, and the repercussions of a one dimensional feedback environment,
 415 see papers by Metz et al. 1996b; Heino et al. 1998; Kisdi 1998; Rueffler et al. 2006; Hoyle and Bowers
 416 2008.)

417

418 By allowing the prey and predator to co-evolve, we show, via numerical simulations, that the predator
 419 can indeed prevent its own extinction. In particular, we initially assume that the predator has a higher
 420 per capita mutation rate than the prey (with a ratio 3:1), potentially allowing the predator to evolve
 421 'faster' than the prey. As β decreases (Figure 6A), given an appropriate trade-off, c increases (Figure
 422 6B). This moves the predator exclusion threshold (6) (and Figure 4) in such a way that it moves below
 423 the pathogen exclusion threshold and therefore as β decreases the pathogen threshold is met first and
 424 the pathogen is excluded (Figure 6C). Again there will exist a singularity just above the pathogen
 425 threshold, however sufficiently large mutations again lead to β crossing the exclusion threshold with I
 426 becoming negligible and the pathogen becoming extinct. In Figure 6D we plot the predator density and
 427 the ratio R_{0P} at evolutionary time step, which remain above 0 and 1 respectively at all times. The
 428 possibility of the above occurring however depends on the predator's optimal evolutionary strategy,
 429 which subsequently optimises $(S + \phi I)$, to be in a region which allows predator survival; if this is not
 430 the case then the predator can not survive no matter how fast it evolves.

431

432 In Figures 6E-H, we plot equivalent results, however in this case we set the per capita mutation rates of
 433 the predator and prey to be equal, such that it would take longer (than previously) for the predator to
 434 decrease its exclusion threshold to a “safe” level to prevent its own extinction. Here the predator does
 435 not evolve enough and the predator exclusion threshold remains above the prey exclusion threshold. In
 436 this case the prey evolves to such a level that β crosses the predator exclusion threshold and the
 437 predator is driven extinct. Again there will exist a singularity very close to the threshold, however
 438 appropriate mutations again lead to the crossing of this threshold and the extinction of the predator. As
 439 was the case in Figures 5A-D, once the predator has been excluded, the system remains in an prey-
 440 infection set-up and the prey evolves to maximise β , and subsequently their birth rate, as there is no
 441 cost in the prey being infected (as there is no castration and no increased death rate, as $\alpha = 0$).
 442
 443
 444



445
 446 Fig. 6: Numerical simulations of the evolution of β for the prey, with a trade-off of the form
 447 $a = f(\beta)$, with $f''(1) = 1.25$, of c for the predator with a trade-off of the form $d = g(c)$, with
 448 $g''(0.05) = -5$ (which we take to have an equivalent form to that in for the prey in (2) with $c^* = 0.05$
 449 and $d^* = 0.3$). Evolution is such that the prey evolves to minimise β and the predator evolves to
 450 maximise c . In (A) and (B) the predator manages to keep its ratio R_{0P} above 1 to allow it to co-exist
 451 with the prey (D); however the pathogen is excluded as its ratio R_{0I} drops below 1 (C). In (E) and (F) the
 452 predator is not able to keep its ratio above 1 and therefore the predator is driven extinct (H); however
 453 the pathogen remains in the environment (G). The parameter values are $q = 0.5$, $b = 0.2$, $\alpha = 0$,
 454 $\gamma = 0.2$, $\theta = 1$, $\phi = 3$, $f'(1) = 0.0935$, $g'(0.05) = 6$.

455
 456

457 6) Discussion

458
459 It is well known that for pathogens to invade and persist commonly requires the host population size to
460 be above a certain threshold, which can generally be derived from the pathogen's reproduction ratio
461 $R_0=1$ (Anderson and May, 1981; Bremermann and Pickering, 1983; Bremermann and Thieme, 1989). In
462 models where pathogen invasion thresholds and exclusion thresholds are coincident, which is the case
463 here, this reproduction ratio can be used to determine the conditions needed for a pathogen to be
464 excluded from a host population. Of interest here is the important problem concerning the conditions
465 under which a host species can evolve in such a way that it falls below this threshold. In the present
466 work, it is seen that evolving greater resistance (at a cost of lowered fecundity) is not sufficient under
467 standard adaptive dynamics analysis (with small, rare mutations) to achieve a state where the
468 population size falls below a level corresponding to $R_0=1$; there is a protective CS singularity preventing
469 this. However, when this singularity is also ES and is sufficiently close to the exclusion boundary, in the
470 realistic case where the mutations are not arbitrarily small, this protection may fail. A mutant which
471 does not itself support the pathogen can arise. Furthermore, this strain can suppress the density of
472 infected hosts to sufficiently low levels that the infection may be lost due to stochastic effects at low
473 population numbers. Subsequently, new mutants that arise will be uninfected and a new evolutionary
474 path will be followed. Such behaviour is seen in the simulations presented here.

475
476 However, as in most previous studies, this result assumes an environment populated by the host and
477 pathogen only, with secondary species/interactions commonly ignored. However in recent years studies
478 at a population level have shown that additional interacting species can have a significant effect on the
479 dynamics of a system (e.g. Greenman and Hoyle, 2010; Haque and Greenhalgh, 2010; Hudson and
480 Greenman, 1998; Haque, 2010; Venturino, 2010), which in turn causes complications for deriving control
481 strategies (Greenman and Hoyle, 2010). These interactions still remain relatively ignored at an
482 evolutionary level. Recent studies by Morozov and Adamson (2011) and Morozov and Best (In Press)
483 have tried to change this, looking at pathogen evolution in an SI model, where a predator feeds on
484 infected prey only. They found that the addition of even a simple predator can change the evolutionary
485 dynamics significantly. This is emphasised even more in the present work where we found an example
486 where, given specific parameter values, the presence of a predator can create the possibility of
487 branching points where none were present previously. Significantly, the way in which the predators
488 affect the exclusion boundaries, $R_0=1$ proves pivotal. Due to the predator, there are now two thresholds
489 $R_{0P}=1$ (number of new infections a single infected prey can make in a completely susceptible
490 environment) and $R_{0P}=1$ (number of offspring a single predator can produce over its lifetime in prey-only
491 environment), where the pathogen and the predator respectively can be excluded (can invade) from a
492 predator-prey-infection environment.

493
494 Although these ratios depend on most of the parameters, a key factor in determining whether the
495 pathogen or predator is excluded first is ϕ , the change in predation experienced by a prey when it
496 becomes infected (Figure 4). A high value of ϕ , where the predator is largely dependent on infected
497 prey for food, led to the predator being excluded first as resistance decreased the number of infected

498 prey and hence the predator's food source; this result echoes that seen by Morozov and Adamson
499 (2011). Subsequent evolution depends on the selection pressures in a prey-only SIS system – for
500 example co-existence of prey and pathogen (Figures 5A-D) or pathogen exclusion (Figure 5E-H). Again,
501 we found exclusion of the parasite requires finite mutations allowing resistance levels to cross the
502 corresponding threshold; however exclusion of predators is found to be possible by host evolution by a
503 parallel mechanism but also in appropriate circumstances by the standard small, rare mutations of
504 adaptive dynamics theory. A low value of ϕ , where the predator mostly consumes uninfected prey, led
505 to the pathogen being excluded first, as resistance drives down the number of infected prey with the
506 predator pushing down the susceptible prey.

507
508 Generally throughout we see that if the predator is present, it can go extinct due to host evolution. In
509 the (final) case where the predator was allowed to co-evolve, it is seen that the predator can prevent its
510 own extinction by evolving in such a way that it lowers its threshold and allows itself to stay above the
511 predator reproduction threshold $R_{op}=1$. In particular we found that the relative per capita mutation rates
512 of the predator and prey are key to whether the predator can persist in the population. The 'speed' of
513 evolution in the two species depends on population sizes, mutation rates and selection gradients
514 (Dieckmann and Law, 1996; Marrow et al., 1996), and we found that if the predator evolves significantly
515 'faster' than the prey due to an increased mutation rate, it was able to shift its extinction threshold
516 sufficiently quickly to prevent the prey driving its extinction. These subtle effects of evolution require
517 further investigation to fully understand the co-evolutionary dynamics.

518
519 A question that is often raised in these systems, especially at a population studies level, is how the
520 behaviour would change if the pathogen could infect both prey and predator. Studies have shown that
521 the resultant behaviour can be more complicated. One population level study by Greenman and Hoyle
522 (2010) showed that the control maps (plots of invasion/exclusion thresholds in 2 parameter space) can
523 become ever more complicated and that exclusion boundaries can become very close together
524 potentially leading to multiple exclusions in quick succession. However more detailed analysis would be
525 needed to determine the effects of shared-pathogens in an evolutionary sense, and, in particular, to
526 investigate whether cross species infection levels would allow for a larger potential pool of susceptibles
527 and make the infection more difficult to exclude, which might perhaps play against the predator.

528
529 Understanding the persistence of pathogens in natural populations is key to the management of many
530 ecological systems. We have shown here how the evolution of host resistance may drive its pathogen to
531 extinction and how the shape of the trade-off between resistance and reproduction is crucial to this
532 possibility. Furthermore, we have shown how this result can be complicated by the presence of an
533 immune predator, considerably changing the evolutionary outcomes and in some cases producing
534 opposite results to when species exist alone (e.g. CS switches to non-CS). This alone provides reason why
535 more studies into complex ecosystems should be carried out. The interactions of all three species can
536 lead to relatively complex evolutionary dynamics, with the shape of the host's trade-off and the relative
537 level of predation experienced by susceptible and infected hosts being key.

538

539 Acknowledgements

540 AH was supported by a Carnegie Research Grant; thanks to Éva Kisdi for some very useful comments.

541

542

543 References

544

545 Anderson, R.M., May, R.M., 1981. The population dynamics of microparasites and their invertebrate
546 hosts. *Phil. Trans. Roy. Soc. Lond. B* 291, 452-524.

547

548 Best, A., White, A., Boots, M., 2009. The implications of co-evolutionary dynamics to host-parasite
549 interactions. *Am. Nat.* 173, 779-791.

550

551 Best, A., White, A., Boots, M., 2010. Resistance is futile but tolerance can explain why parasites do not
552 always castrate their hosts. *Evolution.* 64:348-357.

553

554 Best, A., A. White, Kisdi, É., Antonovics, J., Brockhurst, M., Boots, M., 2010. Evolution of host-parasite
555 range. *Am. Nat.* 176, 63-71.

556

557 Boots, M., Haraguchi, Y., 1999. The evolution of costly resistance in host-parasite systems. *Am. Nat.* 153,
558 359–370.

559

560 Boots, M., Bowers, R.G., 1999. Three mechanisms of host resistance to microparasites - avoidance,
561 recovery and tolerance - show different evolutionary dynamics. *J. Theor. Biol.* 201, 13–23.

562

563 Boots, M., Bowers, R.G., 2004. The evolution of resistance through costly acquired immunity. *Proc. R.*
564 *Soc. London B* 271, 715–723.

565

566 Boots, M., 2008. Fight or learn to live with the consequences? *Trends in Ecol. Evol.* 23, 248-250.

567

568 Boots, M., Best, A., Miller, M. R., White, A., 2009. The role of ecological feedbacks in the evolution of
569 host defence: What does theory tell us? *Phil. Trans. Roy. Soc. Lond. B.* 364, 27-36.

570

571 Bowers, R.G., White, A., Boots, M., Geritz, S.A.H., Kisdi, É., 2003. Evolutionary branching/speciation:
572 contrasting results from systems with explicit or emergent carrying capacities. *Evol. Ecol. Res.* 5, 883-
573 891.

574

575 Bowers R.G., Hoyle, A., White, A., Boots, M., 2005. The geometric theory of adaptive evolution: trade-off
576 and invasion plots. *J. Theor. Biol.* 233, 363-377.

577

578 Bremermann, H.J., Pickering, J., 1983. A game-theoretical model of parasite virulence. *J. Theor. Biol.* 100,
579 411–426.

580

- 581 Bremermann, H.J., Thieme, H., 1989. A competitive exclusion principle for pathogen virulence. *J. Math.*
582 *Biol.* 27, 179–190.
- 583
- 584 de Mazancourt, C., Dieckmann, U., 2004. Trade-off Geometries and Frequency-Dependent Selection.
585 *Am. Nat.* 164, 765-778.
- 586
- 587 Dieckmann, U., Law, R., 1996. The dynamical theory of coevolution: a derivation from stochastic
588 ecological processes. *J. Math. Biol.* 34, 579–612.
- 589
- 590 Dieckmann, U., Metz, J.A.J., Sabelis, M.W., Sigmund, K., 2002. Adaptive dynamics of infectious diseases:
591 In pursuit of virulence management. Cambridge University Press.
- 592
- 593 Frank, S.A., 1993. Co-evolutionary genetics of plants and pathogens. *Evol. Ecol.* 7, 45-75.
- 594
- 595 Geritz, S.A.H., Kisdi, É., Meszéna, G., Metz, J.A.J., 1998. Evolutionary singular strategies and the adaptive
596 growth and branching of the evolutionary tree. *Evol. Ecol.* 12, 35-57.
- 597
- 598 Greenman, J.V., Hoyle, A., 2010. Pathogen exclusion from eco-epidemiological systems. *Am. Nat.* 176,
599 149-158.
- 600
- 601 Haque, M., Zhen, J., Venturino, E., 2009. An epidemiological predator-prey model with standard disease
602 incidence. *Math. Methods App. Sci.*, 32, 875-898.
- 603
- 604 Haque, M. 2010. A predator-prey model with disease in the predator species only. *Nonlinear Analysis:*
605 *Real World Applications*, 11, 2224-2236.
- 606
- 607 Haque, M., Greenhalgh, D., 2010. When a predator avoids infected prey: A model based theoretical
608 study. *Math. Med. Biol.* 27, 75-94
- 609
- 609 Heino, M., Metz, J.A.J, Kaitala, V., 1998. The enigma of frequency-dependent selection. *Trends Ecol.*
610 *Evol.* 13, 367_370.
- 611
- 612 Hoyle, A., Bowers, R.G., 2008. Can possible evolutionary outcomes be determined directly from the
613 population dynamics? *Theor. Pop. Biol.* 74, 311-323.
- 614
- 615 Hoyle, A., Bowers, R.G., White, A., Boots, M., 2008. The influence of trade-off shape on evolutionary
616 behaviour in classical ecological scenarios. *J.Theor. Biol.* 250, 498-511.
- 617
- 618 Hoyle A., R.G. Bowers and A. White, 2011. Evolutionary behaviour, trade-offs and cyclic and chaotic
619 population dynamics. *Bulletin Bull. Math. Biol.*, 73:1154-69.

- 620 Hudson, P., Greenman, J., 1998. Competition mediated by parasites: biological and theoretical progress.
621 Trends in Ecol. & Evol. 13, 387–390.
- 622
- 623 Kisdi, É., 1998. Frequency dependence versus optimization. Trends Ecol. Evol. 13, 508.
- 624
- 625 Kisdi, É., 1999. Evolutionary branching under asymmetric competition. J. Theor. Biol. 197, 149-162.
- 626
- 627 Levin, S., Pimental, D., 1981. Selection of intermediate rates of increase in host-parasite systems. Am.
628 Nat. 117, 308–315.
- 629
- 630 Marrow, P., Dieckmann, U., Law, R., 1996. Evolutionary dynamics of predator-prey systems: an
631 ecological perspective. J. Math. Biol. 34, 556–578.
- 632
- 633 Maynard Smith, J., Price, G.R., 1973. The logic of animal conflict. Nature 246, 15–18.
- 634 Eshel, 1983. Evolutionary and continuous stability. J. Theor. Biol. 103, 99–111.
- 635
- 636 Metz, J.A.J., Geritz, S.A.H., Meszéna, G., Jacobs, F.J.A., Van Heerwaarden, J.S., 1996a. Adaptive dynamics:
637 a geometrical study of the consequences of nearly faithful reproduction. In *Stochastic and Spatial*
638 *Structures of Dynamical Systems* (S.J. Van Strien and S.M. Verduyn Lunel, eds), pp. 183–231. Amsterdam:
639 Elsevier.
- 640
- 641 Metz, J.A.J., Mylius, S.D., Dieckmann, O., 1996b. When does evolution optimise? On the relation between
642 types of density dependence and evolutionarily stable life history parameters. IIASA working paper WP-
643 96-004. Available at: <http://www.iiasa.ac.at/Research/ADN/Series.html>.
- 644
- 645 Miller, M.R., White, A., Boots, M. 2005. The evolution of host resistance: tolerance versus control. J.
646 Theor. Biol. 236, 198-207.
- 647
- 648 Morozov, A. Yu., Adamson, M.W., 2011. Evolution of virulence driven by predator–prey interaction:
649 Possible consequences for population dynamics. J.Theor. Biol. 276, 181-191.
- 650
- 651 Morozov, A. Yu., Best, A. *In Press*. Predation on infected host promotes evolutionary branching of
652 virulence and pathogens' biodiversity. J. Theor. Biol. DOI: 10.1016/j.jtbi.2012.04.023.
- 653
- 654 Pugliese, A., 2002. On the evolutionary co-existence of parasite strains. Math. Biosci. 177-178, 355-375.
- 655
- 656 Restif, O., Koella, J.C., 2003. Shared control of epidemiological traits in a co-evolutionary model of host-
657 parasite interactions. Am. Nat. 161, 827-836.
- 658
- 659 Roy, B.A., Kirchner, J.W., 2000. Evolutionary dynamics of pathogen resistance and tolerance. Evolution
660 54, 51-63.
- 661

- 662 Rueffler, C., Van Dooren, T.J.M., Metz, J.A.J., 2004. Adaptive walks on changing landscapes: Levins'
663 approach extended. *Theor Pop Biol* 65, 165-178.
- 664
- 665 Rueffler, C., Van Dooren, T.J.M., Metz, J.A.J., 2006. The evolution of resource specialization through
666 frequency-dependent and frequency-independent mechanisms. *Am. Nat.* 167, 81_93.
- 667
- 668 Svennungsen, T., and É . Kiski. 2009. Evolutionary branching of virulence in a single-infection model. *J.*
669 *Theor. Biol.* 257, 408–418.
- 670
- 671 van Baalen, M., 1998. Co-evolution of recovery ability and virulence. *Proc. Roy. Soc. B* 265, 317-325.
- 672
- 673 Venturino, E., 2001. The effects of diseases on competing species. *Math. Biosc.*, 174, 111-131.
- 674
- 675 Venturino, E., 2002. Epidemics in predator-prey models: disease in the predators, *IMA J. Math. App.*
676 *Med.Biol.*, 19, 185-205.
- 677
- 678 Venturino, E., 2010. Eco-epidemic models with disease incubation and selective hunting. *J. Comp. App.*
679 *Math.* 234, 2883-2901.
- 680

681 Appendix A – Sign equivalent form of the fitness

682

683 The invasion matrix for the mutant is given by:

684

$$\begin{pmatrix} \hat{a} - qH - b - \hat{\beta}I - cP & \hat{a} - qH + \gamma \\ \hat{\beta}I & -\Gamma - c\phi P \end{pmatrix} = \begin{pmatrix} A & B \\ C & D \end{pmatrix} \quad (\text{A.1})$$

685

686

687 where $B > 0$ (as $a > qH$), $C > 0$ and $D < 0$; the sign of A is unknown. The eigenvalues of the invasion matrix are
688 given by:

689

$$\lambda^+, \lambda^- = 0.5 \left[A + D \pm \sqrt{(A + D)^2 - 4(AD - BC)} \right] = 0.5 \left[A + D \pm \sqrt{(A - D)^2 + 4BC} \right] \quad (\text{A.2})$$

691

692 where the superscript on λ represents the sign taken in solution. The discriminant of these is positive
693 and hence we always have two real eigenvalues.

694

695 As $D < 0$, then it follows that if $A < 0$ then $\lambda^- < 0$; if $A \geq 0$ then it follows that $|A + D| \leq |A - D|$ and therefore that
696 $\lambda^- < 0$. Hence the λ^- eigenvalue will always be negative. In addition it is trivial to show that the other
697 eigenvalue is always larger, i.e. $\lambda^- < \lambda^+$. Therefore we can say that the eigenvalue λ^+ is the maximum
698 eigenvalue and subsequently the fitness of the invading mutant, which we call s .

699

700 As $\lambda^- < 0$, we have two options:

701 1) Non-invasion: $s = \lambda^+ < 0$ and therefore $\det = \lambda^- \lambda^+ > 0$;

702 2) Invasion: $s = \lambda^+ > 0$ and therefore $\det = \lambda^- \lambda^+ < 0$

703 Hence the negative of the determinant is sign equivalent to the fitness, $s = \lambda^+$.

704

705 Appendix B – Trade-off and invasion plots (TIPs)

706

707 The method used in this study is a geometric adaptation of adaptive dynamics, namely that of trade-off
 708 and invasion plots (TIPs) (Bowers et al., 2005). Alternative geometric methods to adaptive dynamics
 709 exist (de Mazancourt and Dieckmann, 2004; Rueffler et al., 2004). The advantage of all of these is that
 710 the trade-off is kept at the forefront, something which is of great interest in this work.

711

712 This method takes the fitness $s(\hat{a}, \hat{\beta}; a, \beta)$ (as given in equation (4)) of a rare mutant strain with
 713 evolving traits $(\hat{a}, \hat{\beta})$ faced with a resident with traits (a, β) . The invasion boundary $\hat{a} = f_1(\hat{\beta}, \beta)$,
 714 between where the mutant can and cannot invade the resident, is determined by $s(\hat{a}, \hat{\beta}; a, \beta) = 0$
 715 (taking $a = f(\beta)$) and here is given by

$$716 \quad f_1(\hat{\beta}, \beta) = qH + \frac{(b + cP)(\Gamma + \phi cP) + \hat{\beta}I(b + \alpha + c\phi P)}{\Gamma + c\phi P + \hat{\beta}I} \quad (\text{B.1})$$

717 A second invasion boundary, $\hat{a} = f_2(\hat{\beta}, \beta)$, can be gained by solving $s(a, \beta; \hat{a}, \hat{\beta}) = 0$, where the roles
 718 of the mutant and resident are reversed. We do not need the explicit form for this at present. These two
 719 curves are plotted in $(\hat{a}, \hat{\beta})$ -space, where (a, β) represents a special point hereby known as an origin.
 720 These invasion boundaries are coincident and tangential at the point $(\hat{a}, \hat{\beta}) = (a, \beta)$.

721

722 The third curve on a TIP is the trade-off curve, $\hat{a} = f(\hat{\beta})$. Evolutionary steps result from constructing
 723 TIPs for varying residents on f . For certain β , the trade-off is also tangential to the invasion
 724 boundaries; these β are the evolutionary singularities, β^* . For our model, differentiating (B.1) with
 725 respect to $\hat{\beta}$ gives

$$726 \quad \frac{\partial f_1}{\partial \hat{\beta}} = \frac{I(\Gamma + c\phi P)(cP(\phi - 1) + \alpha)}{[\Gamma + c\phi P + \hat{\beta}I]^2} \quad (\text{B.2})$$

727 Using the fact that $f'(\beta)$ is tangential to the invasion boundary at $\hat{\beta} = \beta = \beta^*$, from (B.2), and the
 728 equilibrium result $\beta S = \Gamma + c\phi P$, we have

$$729 \quad f'(\beta^*) = \left. \frac{\partial f_1}{\partial \hat{\beta}} \right|_{\beta^*} \Leftrightarrow f'(\beta^*) = \frac{S^* I^* (cP^* (\phi - 1) + \alpha)}{\beta^* H^{*2}} \quad (\text{B.3})$$

730 To determine the nature of an evolutionary singularity we use the relative curvatures (or shapes) of the
 731 three curves at a singularity. The invasion boundaries determine which types of evolutionary
 732 singularities are possible and the trade-off determines which actually occurs.

733

734 To determine the evolutionary stability or ES boundary (Maynard Smith, 1973), we require the locally
 735 possible mutants – those on the trade-off – to be on the appropriate side of the ES (invasion) boundary

736 f_1 . Differentiating (B.2) with respect to $\hat{\beta}$, evaluating at a singularity $\hat{\beta} = \beta = \beta^*$ and using
 737 $\beta S = \Gamma + c\phi P$, gives the right hand side of (A.4) and hence the ES condition as

$$738 \quad ES \Leftrightarrow \lambda f''(\beta^*) < \lambda \left. \frac{\partial^2 f_1}{\partial \hat{\beta}^2} \right|_{\hat{\beta}=\beta=\beta^*} \Rightarrow f''(\beta^*) < -\frac{2S^* I^{*2} (cP^* (\phi-1) + \alpha)}{\beta^{*2} H^{*3}} \quad (B.4)$$

739 where $\lambda = \text{sign}\left(\partial s(\hat{a}, \hat{\beta}; a, \beta) / \partial \hat{a}\big|_{\beta^*}\right) = 1$ in our examples.

740

741 To determine whether the singularity is convergent stable or CS (Eshel, 1983), we need to ensure that
 742 the species evolves towards the singularity. The boundary for this is gained by constructing a fourth
 743 curve by taking the mean coordinates of f_1 and f_2 at each value of $\hat{\beta}$. At the evolutionary singularity
 744 this curve has the same gradient as f_1 and f_2 ; furthermore its curvature is the mean of that of f_1 and
 745 f_2 (Bowers et al., 2005). Hence to be CS the mutants must be on the appropriate side of the boundary
 746 and therefore

$$747 \quad CS \Leftrightarrow \lambda f''(\beta^*) < \frac{\lambda}{2} \left(\left. \frac{\partial^2 f_1}{\partial \hat{\beta}^2} + \frac{\partial^2 f_2}{\partial \hat{\beta}^2} \right) \right) \bigg|_{\hat{\beta}=\beta=\beta^*} \quad (B.5)$$

748 The curvature of the f_2 boundary at a singularity can be calculated using the curvature of f_1 and the
 749 mixed derivative of f_1 (Bowers et al., 2005) in the form

$$750 \quad \left. \frac{\partial^2 f_2}{\partial \hat{\beta}^2} \right|_{\beta^*} = \left. \frac{\partial^2 f_1}{\partial \hat{\beta}^2} \right|_{\beta^*} + 2 \left. \frac{\partial^2 f_1}{\partial \beta \partial \hat{\beta}} \right|_{\beta^*} \quad (B.6)$$

751 Calculating the mixed derivative of f_1 , by differentiating (B.2) with respect to β and evaluating at a
 752 singularity, and using $\beta S = \Gamma + c\phi P$ and (B.3), gives

$$753 \quad \left. \frac{\partial^2 f_1}{\partial \beta \partial \hat{\beta}} \right|_{\beta^*} = \frac{\partial I}{\partial \beta} \frac{S(cP(\phi-1) + \alpha)(S-I)}{\beta H^3} + \frac{cI}{\beta^2 H^3} \frac{\partial P}{\partial \beta} [-\phi(cP(\phi-1) + \alpha)(S-I) + \beta SH(\phi-1)] \quad (B.7)$$

754

755 Predator-free environment

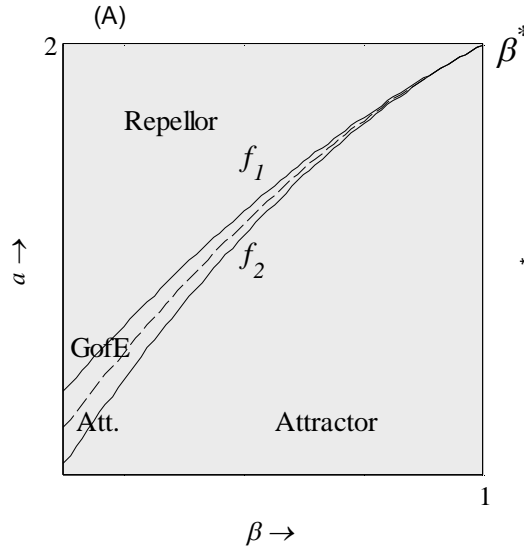
756 To explore this further, we first look at the case where the prey exists in a predator free environment,
 757 hence $P = 0$ and $\partial P / \partial \beta = 0$. The derivative of the susceptible population is $\partial S / \partial \beta = -S / \beta$, as
 758 $S = \Gamma / \beta$. Differentiating dH/dt in (1) through with respect to β , evaluating at equilibrium and solving
 759 for $\partial I / \partial \beta = 0$, using (B.3) gives

760

$$761 \quad \left. \frac{\partial I}{\partial \beta} \right|_{\beta^*} = \frac{qSH^2}{\beta(qH^2 + \alpha S)} \Rightarrow \left. \frac{\partial^2 f_1}{\partial \beta \partial \hat{\beta}} \right|_{\beta^*} = \frac{\alpha qS^2 H^2 (S-I)}{\beta^2 H^3 (qH^2 + \alpha S)} \quad (B.10)$$

762 We can put this, and the curvature of f_1 from (B.4), into (B.6) to get the curvature of f_2 , and hence use
 763 (B.5) to get the CS condition. Combinations of ES and CS determine the nature of the evolutionary
 764 singularity (Metz et al., 1996a; Geritz et al., 1998; Bowers et al., 2005).

765
 766 An example of how the invasion boundaries appear when plotted on a singular TIP is given in Fig. B.1.
 767



768
 769 Fig. B.1: A typical Trade-off and Invasion Plot for a trade-off between reproduction a and transmission
 770 β . Branching points are not possible for this plot as the f_1 invasion boundary is above the f_2 so that a
 771 region where the singularity is CS but not ES does not occur. (If the two invasion boundaries were
 772 swapped over then the Garden of Eden (ES-repellor) region would be replaced by a branching region.)
 773 The parameter values are $q = 0.5$, $b = 0.2$, $\alpha = 0.2$, $\gamma = 0.2$, $c = 0$, $a^* = 2$, $\beta^* = 1$.

774
 775
 776 Predator-prey-infection
 777 To gain the results for Fig. 3, we require the CS condition for when both the predator and the infection
 778 are present, i.e. when $P > 0$ (and hence $\theta c(S + \phi I) - d = 0$) and $I > 0$ (and hence
 779 $\beta S - \Gamma - c\phi P = 0$). Returning to the original dynamical equations in (1) and differentiating the

780 predator and infection equations through with respect to β we can find the derivatives of S and P as

$$781 \quad \frac{\partial S}{\partial \beta} = -\phi \frac{\partial I}{\partial \beta} \quad \text{and} \quad \frac{\partial P}{\partial \beta} = \frac{S}{\phi c} - \frac{\beta}{c} \frac{\partial I}{\partial \beta} \quad (\text{B.9})$$

782 Differentiating the dynamical equation for the total prey population gives

$$783 \quad \frac{\partial}{\partial \beta} \left(\frac{dH}{dt} \right) = \frac{da}{d\beta} H + \frac{\partial H}{\partial \beta} (a - 2qH - b) - \alpha \frac{\partial I}{\partial \beta} - c \frac{\partial P}{\partial \beta} (S + \phi I) + cP \left(\frac{\partial S}{\partial \beta} + \phi \frac{\partial I}{\partial \beta} \right) = 0 \quad (\text{B.10})$$

784 Evaluating at an evolutionary singularity, and hence using (A.3) for $da/d\beta$ (and solving for $\partial I / \partial \beta$), we
 785 get

$$786 \quad \frac{\partial I}{\partial \beta} = \frac{S(-\phi I(cP(\phi-1)+\alpha) + \beta H(S + \phi I))}{\phi \beta H[(a - 2qH - b)(1-\phi) - \alpha + \beta(S + \phi I)]} \quad (B.11)$$

787 Substituting (A.9) into the mixed derivative from (A.8) gives

$$788 \quad \left. \frac{\partial^2 f_1}{\partial \beta \partial \hat{\beta}} \right|_{\beta^*} = \frac{1}{\beta H^3} \frac{\partial I}{\partial \beta} [(S + \phi I)(cP(\phi-1) + \alpha)(S - I) - \beta SIH(\phi-1)] \\ + \frac{SI}{\phi \beta^2 H^3} [-\phi(cP(\phi-1) + \alpha)(S - I) + \beta SH(\phi-1)] \quad (B.12)$$

789

790 Appendix C – Numerical Simulations

791

792 Simulation analysis is used to verify the theoretical results about the position and nature of the singular
 793 point. In the simulations, the population dynamics were numerically solved for a fixed time (t_a)
 794 according to (1) initially with a monomorphic population. Mutant strains, those we defined by trait
 795 values $\hat{\beta}$ (and $\hat{a} = f(\hat{\beta})$), were generated by small deviations around the current trait β
 796 (and $a = f(\beta)$) (the choice of current strain from which to mutate depends on its relative density) and
 797 introduced at low density. The population dynamics were then solved for a further time t_a with strains
 798 whose total population density fell below a (very low) threshold considered extinct and removed; in
 799 addition, and a new feature for this study, if the total infection (predator) level across all strains fell
 800 below this threshold, the pathogen (predator) was considered extinct and removed, but the susceptible
 801 counterparts remain. After this removal, new mutations were created and the procedure repeats. In this
 802 way, the parameter β (and therefore a via the trade-off) could evolve. One difference between the
 803 theory and simulations is that the simulations are not mutation-limited (i.e. new mutants could evolve
 804 before previous mutants had reached equilibrium or gone extinct). Although this could be overcome by
 805 increasing t_a , this set-up has generally been shown to correctly approximate the evolutionary behaviour
 806 predicted by adaptive dynamics in studies where the dynamical attractor is an equilibrium point (see, for
 807 example, Hoyle et al. 2011).

808

809 Appendix D - Discontinuity in the CS condition

810

811 By combining (B.9) and (B.11), it can be shown that as c goes towards the critical value that allows the
 812 predator to invade from above, and hence as $P \rightarrow 0^+$, the derivative $\partial S / \partial \beta$ does not equal the
 813 equivalent derivative if you were to approach that same point from the other direction (see result near
 814 (B.7)):

$$815 \quad \left. \frac{\partial S}{\partial \beta} \right|_{P \rightarrow 0^+} = -\frac{S}{\beta} \frac{-\phi I \alpha + \beta H(S + \phi I)}{H[(a - 2qH - b)(1-\phi) - \alpha + \beta(S + \phi I)]} \neq \left. \frac{\partial S}{\partial \beta} \right|_{P \rightarrow 0^-} = -\frac{S}{\beta} \quad (D.1)$$